Effect of annealing temperature on structural and optical properties of ZnO thin films deposited by spin coating method for optoelectronic devices applications

S. NITHYA, R. SENGODAN*
Department of Physics, Kumaraguru College of Technology, Coimbatore-49, India

Zinc oxide thin films were deposited on thoroughly cleaned glass substrates using the spin coating technique and subsequently characterized by X-ray diffraction (XRD) and UV–Vis spectroscopy. The XRD patterns confirmed the formation of a hexagonal wurtzite crystal structure, with crystallite size found to increase progressively with annealing temperature, reflecting improved crystallinity. Structural parameters such as dislocation density and macrostrain were also evaluated and are reported in this study. UV–Vis spectroscopy studies reveal the film's optical parameters, which provided insights into transmittance, absorption coefficient, and extinction coefficient. The optical band gap was determined from the absorption spectra, with values ranging from 2.60 eV for the as-deposited film to 2.22 eV for the film annealed at 400 °C. The observed reduction in band gap with increasing annealing temperature is attributed to decreased defect density and enhanced crystallinity.

(Received October 10, 2025; accepted April 6, 2026)

Keywords: Spin coating, XRD, UV-Vis Spectroscopy

1. Introduction

Zinc oxide (ZnO) is an II–VI compound semiconductor with a wide direct band gap of 3.3 eV, a large excitonic binding energy, high carrier mobility, and excellent thermal, mechanical, and chemical stability. These intrinsic properties, along with its low resistivity and strong electrochemical coupling coefficient, make ZnO a promising material for electronics, optoelectronics, and laser technologies. Furthermore, ZnO exhibits multifunctional characteristics such as broad ultraviolet absorption, biocompatibility, biodegradability, and piezoelectric and pyroelectric effects, thereby broadening its applicability in biomedical sciences, sensing, and energy harvesting [1–4].

Crystallizing in the hexagonal wurtzite structure (lattice parameters a = 3.253 Å, c = 5.215 Å), ZnO has been successfully applied in photocatalysis, spintronic devices, gas sensors, voltage-dependent resistor, light-emitting diodes, and lasers. Its strong piezoelectric response has led to applications in converters, sensors, energy generators, and surface acoustic wave (SAW) devices. In photovoltaics, ZnO thin films are commonly employed as transparent conducting oxides or window layers in both polycrystalline and thin-film silicon solar cells [5]. In addition, ZnO nanostructures can be grown in one-, two-, and three-dimensional forms, providing versatile platforms for nanotechnology-driven applications [6].

Several deposition methods have been explored to fabricate ZnO thin films, including sol–gel processing, sputtering, chemical vapor deposition, spray pyrolysis, molecular beam epitaxy and pulsed laser deposition (PLD) [7–10]. The spin coating technique is widely preferred due to its simplicity, low cost, vacuum-free processing, and precise control over film composition and thickness.

Multicomponent oxide layers are fabricated on a glass substrate covering large area [11]. The properties influencing the synthesized sol-gel ZnO films are sol aging time [12], film thickness [13], and post-deposition annealing treatment [14]. The removal of organic residues can be achieved by annealing which in turn enhances the grain growth and reducing defect density.

This research work focuses on the structural modifications and optical properties of annealed zinc oxide thin films. From the obtained results it is suggested that Zinc oxide thin films are suitable for optoelectronic device applications.

2. Experimental technique

2.1. Materials and methods

Zinc oxide (ZnO, Merck, 1 g) was dissolved in 25 mL of ethanol at room temperature and stirred for 3 hours to obtain a homogeneous solution. The glass substrate was cleaned by using soap solution and rinsed with distilled water in order to remove surface contaminants. Once the substrate is cleaned moisture content is removed from the substrate by heating at 100 °C for 1 hour. ZnO thin films are coated by spin coating technique with 2400 rpm for 50 seconds. The uniformly coated thin films are annealed in air at different temperatures 100 °C, 250 °C and 400 °C for 1 hour. The effect of annealing on structural and optical characteristics is studied. The annealing temperatures of 100 °C, 250 °C, and 400 °C were selected to systematically investigate the thermal evolution of ZnO thin films from

low-temperature solvent removal to enhanced crystallization. The temperature of 100 °C facilitates the evaporation of residual solvents and moisture, 250 °C promotes the decomposition of remaining organic species and initiates grain growth, while 400 °C enhances crystallinity and defect reduction without causing film degradation or substrate damage. These temperature values are also consistent with commonly reported annealing ranges for sol–gel-derived ZnO thin films.

2.2. Characterization

2.2.1. Structural analysis

Bruker AXS D8 Advance diffractometer was used to record diffraction pattern of thin films ranging from 10° to 80°, with Cu Kα radiation (λ = 1.5406 Å), operated at a current of 30 mA and accelerating voltage of 40 kV.

2.2.2. UV-visible-NIR spectrophotometry

UV–Vis–NIR spectrophotometer (JASCO V-670, Japan) was used to study the films' optical properties. The evaluation was carried out in the wavelength range of 350–2500 nm with a spectral resolution of 0.1 nm.

3. Result and discussion

3.1. X-ray diffraction analysis

X-ray diffraction (XRD) analysis revealed notable modifications in crystallographic properties due to annealing. The diffraction peaks appearing at 2θ ≈ 31.25°, 33.87°, 35.85°, 44.5°, 56.15°, 62.42°, and 67.5° were indexed to the (100), (002), (101), (102), (110), (013), and (112) planes, respectively, confirming the formation of a hexagonal wurtzite structure [15].

The diffraction peaks recorded at room temperature are of less intense indicating decrease in crystal size due to lattice strain. Annealing at 100 °C exhibited improved sharpness and intensity indicating the onset of grain growth and defect reduction. A further increase in annealing temperature to 250 °C results in a significant enhancement of the (002) reflection, demonstrating the development of strong preferential orientation along the c-axis [16]. At 400 °C, the diffraction peaks reach maximum sharpness and intensity, confirming well-developed crystallinity, larger crystallite size, and stress relaxation within the lattice [17]. Notably, the dominance of the (002) reflection at higher temperatures highlights the preferential c-axis orientation of the crystallites, while the absence of additional peaks confirms that no secondary phases are formed during the annealing process [16].

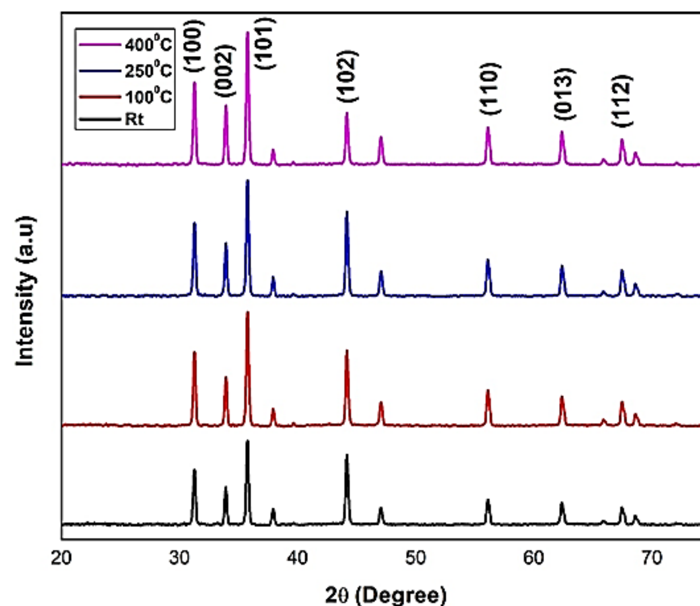

Fig. 1. X-ray diffractograms versus wavelength ZnO thin films (colour online)

The structural parameters of ZnO thin films annealed at different temperatures were determined from XRD data using standard relations for crystallite size, dislocation density, and microstrain, and the results are summarized in Table 1.

Table 1. Structural parameters of ZnO thin films

Sample name	Crystallite size (D) (nm)	Dislocation density 10^{15} lines/m^2	D Spacing (Å)	Estimated strain 10^{-3}
Room temperature	32.6004	0.966507	2.0233	2.761736
100^0C	32.6463	0.964373	2.0237	2.754009
250^0C	32.6766	0.966241	2.0234	2.755752
400^0C	32.7658	0.957626	2.0233	2.743992

The average crystallite size (D) was calculated using the Scherrer's formula [18]

$$D=\frac{K\lambda}{\beta\cos\theta} \quad (1)$$

β – Full width half maximum of the corresponding XRD peak at radiant.
K – constant (≈0.94).
θ – Bragg's angle
λ – wavelength of X-ray

The dislocation density (δ), which represents the number of defects in the crystal, is estimated from the equation,

$$\delta = \frac{1}{D^2} \quad (2)$$

Strain (ε) of the thin film is determined from the following formula

$$\varepsilon = \frac{\beta\cos\theta}{4} \quad (3)$$

Table 1 indicates that the average crystallite size (D) was found to increase slightly from 32.60 nm at room temperature to 32.76 nm at 400 °C, which indicates modest grain growth upon annealing. Correspondingly, the dislocation density (δ), which is inversely proportional to crystallite size squared, decreased from 0.9665 × 10^{15} lines/m^2 at room temperature to 0.9576 × 10^{15} lines/m^2 at 400 °C, reflecting a reduction in crystal imperfections and lattice defects. The d-spacing remained nearly constant (~2.023 Å) across all temperatures, confirming that the hexagonal wurtzite lattice is structurally stable during annealing. However, the estimated microstrain (ε) decreased gradually from 2.76 × 10^{-3} at room temperature to 2.74 × 10^{-3} at 400 °C, suggesting a relaxation of internal stresses with increasing annealing temperature. These observations are in good agreement with recent reports that annealing enhances crystallinity by reducing lattice imperfections and strain while promoting a mild increase in crystallite size without altering the basic wurtzite structure [19,20].

3.2. Optical properties

The transmittance spectra of ZnO thin films are shown in Fig. 2. A clear trend of enhanced transmittance with increasing annealing temperature is observed, with the room-temperature (RT) film exhibiting the lowest transparency across the measured wavelength range. This reduced transmittance in the as-deposited state is commonly attributed to the presence of a high density of structural defects, lattice disorder, and residual impurities, which promote both light scattering and sub-bandgap absorption [21,22]. Upon thermal annealing, the films demonstrate a significant improvement in optical transparency, particularly in the visible and near-infrared regions, where transmittance values above 70% are achieved for the film annealed at 400 °C [23]. The enhancement in transmittance can be ascribed to improved crystallinity, grain growth, and a reduction in native point defects such as oxygen vacancies and zinc interstitials, which introduce localized electronic states within the band gap and thereby increase optical absorption [24]. Furthermore, annealing contributes to film densification and the relaxation of residual stresses, resulting in a more uniform and defect-free microstructure that favours higher optical transmission [25]. These findings are consistent with previous reports on thermally treated Zinc oxide thin films, which showed improved structural and optical properties. Overall, the observed increase in transmittance with annealing temperature highlights the crucial role of post-deposition thermal treatment in optimizing ZnO thin films for applications in optoelectronic devices, transparent conducting electrodes, and solar cell window layers.

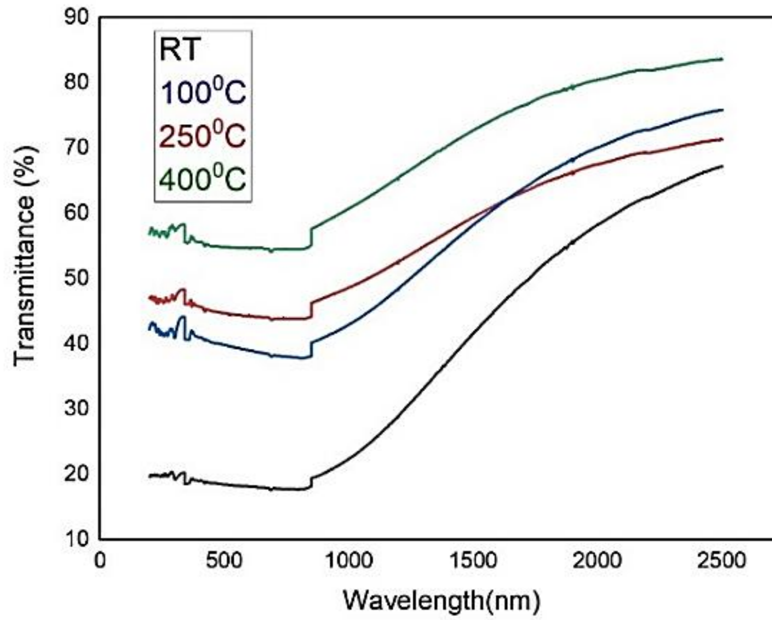

Fig. 2. Transmittance versus wavelength of the ZnO thin films (colour online)

From the transmittance data, the extinction coefficient (k) was calculated using the following relation (4).

$$k = \frac{2.303\, log_{10}\left(\frac{1}{T}\right)\lambda}{4\pi t} \tag{4}$$

where t is the thickness of film and T is the transmittance

The absorption coefficient (α) was calculated using the following relation.

$$\alpha = \frac{4\pi k}{\lambda} \tag{5}$$

where λ is the wavelength of the incident radiation and k is the extinction coefficient. The absorption coefficient is related to energy gap by

$$\alpha \propto \left[h\upsilon - E_g\right]^m \tag{6}$$

In this relation, the value of m is taken as 2 for indirect transitions and 1/2 for direct transitions. Among the fundamental optical parameters, the refractive index holds particular importance, as it is wavelength-dependent and governs the interaction of electromagnetic radiation with the material. When light propagates through a medium, it may undergo various losses arising from free carrier absorption, photon scattering and phonon interactions (lattice vibrations). In integrated optics, the refractive index represents an important parameter in shaping both the design and operational efficiency of component including waveguides, switches, and filters, as it dictates the propagation and confinement of light within the device. It is also a key parameter in electrochromic systems, where changes in refractive index contribute to voltage-induced variations in color or transparency. For thin film analysis, the Swanepoel method is widely recognized as a reliable and precise approach for extracting the refractive index, with the corresponding relation expressed as follows [26].

$$n = [H + (H^2 + S^2)^{1/2}]^{1/2} \tag{7}$$

where H is the Swanepoel coefficient

$$H = \frac{4S^2}{(S^2+1)T^2} - \frac{S^2+1}{2} \tag{8}$$

where s is the refractive index of the substrate (1.5 for glass) and T is the interference free transmittance

The extinction coefficient (k) spectra of ZnO thin films are shown in Fig. 3. The as-deposited film at room temperature exhibits the lowest k values (~0.1–0.2) across the investigated wavelength range, indicating weak light attenuation within the film. With increasing annealing temperature, the extinction coefficient systematically increases, reaching a maximum value of ~0.8 at 400 °C. In the ultraviolet region, a sharp rise in k corresponds to the fundamental absorption edge of ZnO near 375 nm (~3.3 eV). The increase in k with annealing temperature can be correlated with improved crystallinity and enhanced band-to-band absorption, as thermal treatment reduces structural defects and disorder, thereby sharpening the absorption edge [27, 28]. While the RT film shows low k values, this is primarily due to defect-induced scattering rather than intrinsic absorption, which simultaneously lowers transmittance. In contrast, annealed films exhibit stronger intrinsic optical absorption with higher k values, consistent with the reduction of sub-bandgap defect states and improved optical transition probabilities [29,30]. These findings complement the transmittance and absorption coefficient analyses (Figures 1 and 2), collectively confirming that post-deposition annealing enhances the

optical constants of ZnO thin films and improves their suitability for optoelectronic and transparent conducting applications.

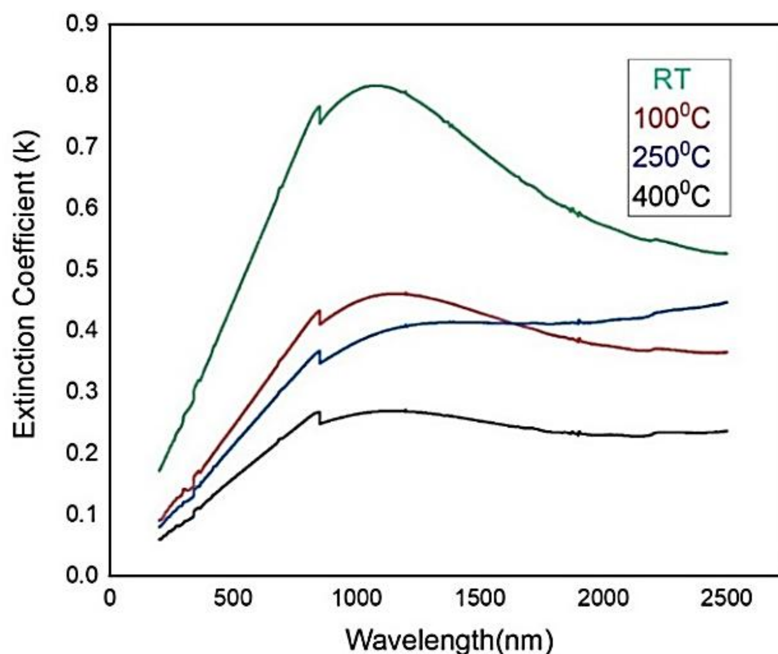

Fig. 3. Extinction coefficient versus wavelength of ZnO thin films (colour online)

Fig. 4 illustrates the dependence of the absorption coefficient (α) on wavelength for ZnO thin films. The as-deposited film at room temperature exhibits the highest absorption coefficient across the investigated spectral range, with values exceeding 1.2×10^7 cm^{-1} in the ultraviolet region. Such pronounced absorption is associated with the presence of structural defects, lattice disorder, zinc interstitials, and oxygen vacancies, which generate sub-bandgap states and enhance defect-related optical transitions [27]. As the annealing temperature increases, the absorption coefficient progressively decreases, and the absorption edge becomes more distinct by a sharper absorption edge near the fundamental band gap of ZnO (~3.3 eV, ~375 nm). Similar trends have been reported by Sanjeev and Kekuda [28] and Husna et al. [30], who demonstrated that thermal annealing reduces defect density and improves optical quality. The reduction in α for the films annealed at 100 °C, 250 °C, and particularly 400 °C indicates improved crystallinity, grain growth, and the removal of defect states that otherwise promote parasitic absorption in the visible and near-infrared regions [23]. Furthermore, annealing contributes to film densification and stress relaxation, suppressing non-radiative recombination centers and minimizing light scattering, in agreement with observations by Suvorova et al. [29]. Although the extinction coefficient (k) shows an increase near the fundamental absorption edge with annealing temperature, the overall absorption coefficient (α) in the visible region decreases. This apparent contradiction arises because annealing improves crystallinity and sharpens the intrinsic band-to-band absorption edge, leading to a localized increase in k in the ultraviolet region. Simultaneously, defect-related sub-bandgap absorption and light scattering are reduced due to improved structural quality and defect removal, resulting in a lower overall absorption coefficient in the visible range. Thus, annealing enhances intrinsic absorption behaviour while suppressing defect-induced optical losses. These findings align with the transmittance spectra shown in Fig. 1, indicating that thermal treatment significantly improves the optical quality of Zinc oxide thin films, best suited for transparent and optoelectronic device applications.

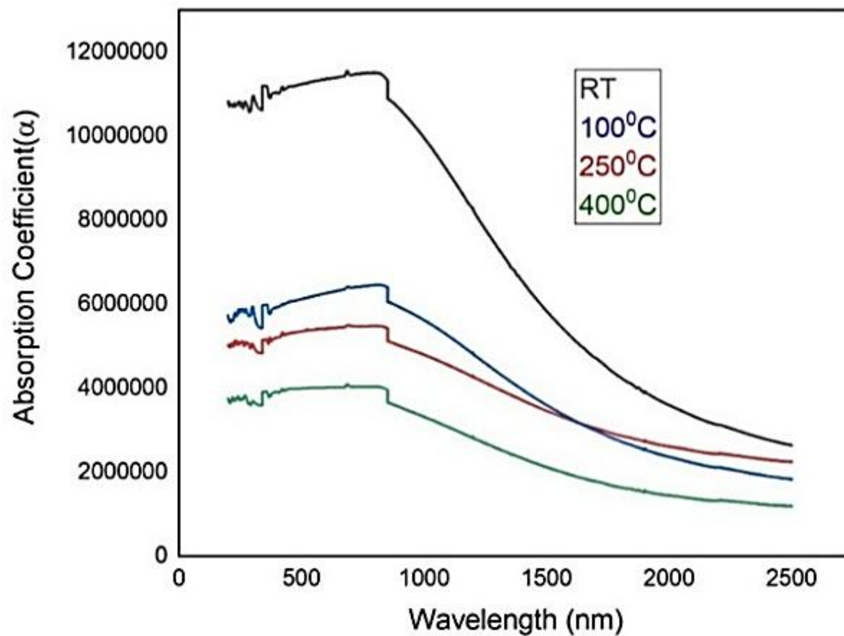

Fig. 4. Absorption coefficient versus wavelength of ZnO thin films (colour online)

The optical band gap (Eg) values of the ZnO thin films were evaluated using the Tauc relation, $(\alpha h\nu)^2=A(h\nu-E_g)$ (Fig. 5). The Tauc plots were constructed assuming a direct allowed transition (m=1/2) as ZnO is a well-known direct band gap semiconductor with a direct transition energy of approximately 3.3 eV in its bulk form. The hexagonal wurtzite structure of ZnO supports direct electronic transitions at the point of the Brillouin zone. Therefore, the, (αhν)2 versus hν relationship was employed to determine the optical band gap in accordance with the established optical transition mechanism of ZnO The calculated band gap values are presented in Table 2. A distinct decreasing trend in Eg with increasing annealing temperature is evident, with the room-temperature (RT) film exhibiting the highest band gap of 2.60 eV, which gradually decreases to 2.22 eV for the film annealed at 400 °C [11]. The optical band gap values obtained in this study are lower than the intrinsic bulk ZnO band gap (~3.3 eV). This reduction can be attributed to defect-induced band tailing arising from oxygen vacancies, zinc interstitials, and structural disorder in sol–gel-derived ZnO thin films. These defect states introduce localized energy levels within the band gap, resulting in a shift of the absorption edge toward lower photon energies. Additionally, minor deviations may arise from limitations of the Tauc extrapolation method and thickness-related light scattering effects in polycrystalline films.

With annealing, defect density decreases, carrier concentration reduces, and the band gap narrows toward its intrinsic value [23,28]. Additionally, improvements in crystallinity and grain growth with annealing contribute to the observed decrease in band gap energy [25,27,31].

These findings align well with the observed variations in transmittance, absorption coefficient, extinction coefficient, and refractive index, exploring that the annealing plays a vital role in effectively tailoring the optical properties of Zinc Oxide thin films.

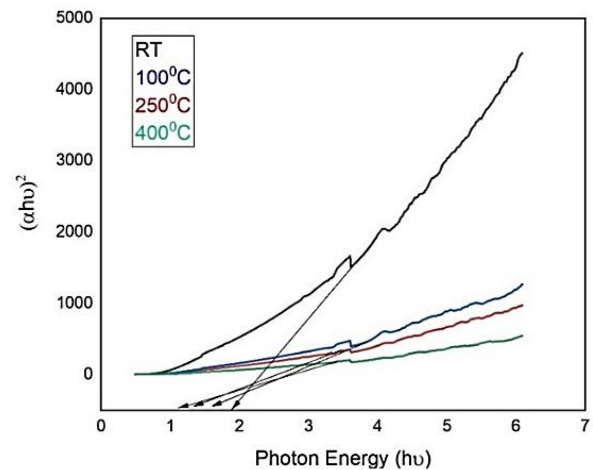

Fig. 5. $(\alpha h\nu)^2$ versus photon energy (hν)

Table 2. Band gap ZnO thin films (colour online)

Temperature (^{0}C)	Band gap (eV)
Room temperature	2.6
100	2.52
250	2.36
400	2.22

The refractive index (n) spectra of ZnO thin films annealed at different temperatures are presented in Fig. 6.

The as-deposited film at room temperature exhibits the highest refractive index, with values exceeding 12 in the ultraviolet region and gradually decreasing toward longer wavelengths. This abnormally high refractive index at RT can be attributed to poor crystallinity, high defect density,

and inhomogeneous microstructure, which enhance light scattering and contribute to anomalous dispersion behaviour [27]. With increasing annealing temperature, the refractive index decreases systematically, stabilizing at ~3–4 in the visible region for the samples annealed at 250 °C and 400 °C. The reduction in n upon annealing is associated with improved structural quality, grain growth, and the removal of lattice imperfections and residual stresses, which results in a more compact and homogeneous film [23, 28]. Moreover, the observed normal dispersion behaviour at higher annealing temperatures reflects a sharper absorption edge and reduced defect-related optical transitions, consistent with the extinction coefficient and absorption coefficient analyses (Figs. 2 and 3).

The findings indicate that thermal annealing enhances the transparency of Zinc oxide thin films while simultaneously modifying their refractive index, optimizing them for applications in sensors, antireflection coatings, and transparent conductive layers [29,30].

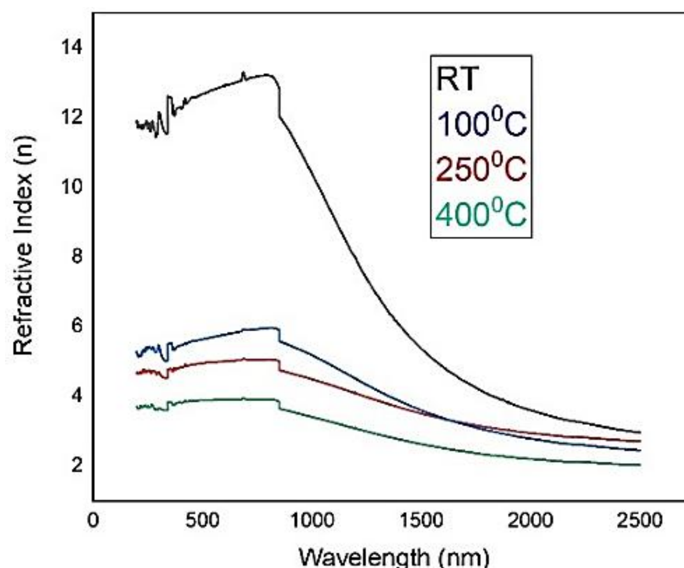

Fig. 6. Refractive index versus wavelength of ZnO thin films (colour online)

4. Conclusion

Structural and optical properties of zinc oxide thin films deposited by spin coating technique at different annealing temperatures were studied. From XRD data, it is observed that the annealed film exhibits more intense and sharp diffraction peaks than the film deposited at room temperature thereby increasing crystalline size and grain growth. The transmittance spectra shows that the transmittance increases with increasing annealing temperature. Concurrently, the optical energy gap and refractive index were found to decrease with annealing, consistent with the reduction of structural defects and relaxation of residual stresses. Overall, the ZnO thin films exhibited excellent transparency, low absorbance, and a polycrystalline nature, underscoring their potential as promising candidates for transparent optoelectronic device applications such as solar cell window layers, light-emitting devices, and optical coatings.

References

[1] G. Balakrishnan, V. Sinha, Y. Palai Peethala, M. Kumar, R. Golden, R. J. Nimal, J. H. Hussain, K. M. Batoo, E. H. Raslan, Materials Science-Poland **38**(1), 17 (2020).
[2] C. M. Raghavan, J. W. Kim, K. W. Jang, S. S. Kim, Journal of the Korean Physical Society **66**(7), 1045 (2015).
[3] S. T. Shishiyanu, T. S. Shishiyanu, O. I. Lupen, Sensors and Actuators B: Chemical **107**(1), 379 (2015).
[4] E. Suvaci, I. O. Ozer, Journal of the European Ceramic Society **25**(10), 1663 (2005).
[5] M. H. Huang, S. Mao, H. Feick, H. Yan, Y. Wu, H. Kind, E. Weber, R. Russo, P. Yang, Science **292**(5523), 1897 (2001).
[6] A. Kołodziejczak-Radzimska, T. Jesionowski, Materials **7**(4), 2833 (2014).
[7] S. Agrawal, R. Rane, S. Mukherjee, Conference Papers in Energy, Hindawi Publishing Corporation, 123456 (2013).
[8] M. Caglar, Y. Caglar, S. Ilican, J. Optoelectron. Adv. M. **8**(4), 1410 (2006).
[9] H. W. Kim, N. Kim, C. Lee, Journal of the Korean Physical Society **44**(1), 14 (2004).
[10] S. Ilican, Y. Caglar, M. Caglar, J. Optoelectron. Adv. M. **10**(10), 2578 (2008).
[11] O. Khanali, K. Nekouee, Synthesis and Sintering **5**(2), 93 (2025).
[12] Y. Li, L. Xu, X. Li, X. Shen, A. Wang, Applied Surface Science **256**(14), 4543 (2010).
[13] M. A. Yildirim, A. Ates, Optics Communications **283**(7), 1370 (2010).

[14] Y. C. Liu, S. K. Tung, J. H. Hsieh, Journal of Crystal Growth **287**(1), 105 (2006).
[15] Theopolina Amakali, Likius. S. Daniel, Veikko Uahengo Nelson Y. Dzade, Nora H. de Leeuw, Crystals **132**, 1 (2020).
[16] P. Sharma, K. Sreenivas, K. V. Rao, Thin Solid Films **445**(1), 20 (2003).
[17] C. D. Lokhande, D. P. Dubal, O. S. Joo, Current Applied Physics **11**(3), 255 (2011).
[18] R. Sengodan, B. Chandar Shekar Bellan, J. Optoelectron. Adv. M. **22**(5-6), 280 (2020).
[19] Adil Alshoaibi, Inorganics **12**, 236 (2024).
[20] Ghaida M. Wazzan, Jwaher M. AlGhamdi, Nuhu Dalhat Muazu, Tarek Said Kayed, Emre Cevik, Khaled A. Elsayed, Catalysts **15**, 71 (2025).
[21] S. Sanjeev, D. Kekuda, IOP Conf. Ser.: Mater. Sci. Eng. **3**(1), 012149 (2015).
[22] Sathish Sugumaran, Chandar Shekar Bellan, Dinesh Muthu, Sengodan Raja, Dinesh Bheemane, Ranjithkumar Rajamani, RSC Adv. **5**, 10599 (2015).
[23] Q. Lin, F. Zhang, N. Zhao, P. Yang, Micromachines **13**(2), 296 (2022).
[24] S. Nithya, R. Sengodan, J. Optoelectron. Adv. M. **26**(5–6), 246 (2024).
[25] N. A. Suvorova, I. O. Usov, L. Stan, R. F. DePaula, A. M. Dattelbaum, Q. X. Jia, A. A. Suvorova, Appl. Phys. Lett. **92**, 141911 (2008).
[26] Arul Carolin Amala, Ravi Vignesh, Gopalakrishnan Vasanthi Geetha, Rengasamy Sivakumar, Phys. Status Solidi A **2100282**, 1 (2021).
[27] M. R. Alenezi, A. S. Alshammari, N. Aljaafari, S. J. Henley, Thin Solid Films **519**(11), 4155 (2011).
[28] S. Sanjeev, D. Kekuda, IOP Conf. Ser.: Mater. Sci. Eng. **73**, 012149 (2015).
[29] N. A. Suvorova, I. O. Usov, L. Stan, R. F. DePaula, A. M. Dattelbaum, Q. X. Jia, A. A. Suvorova, Appl. Phys. Lett. **92**, 141911 (2008).
[30] J. Husna, M. R. Johan, A. A. Aziz, A. Kassim, Procedia Engineering **41**, 1367 (2012).
[31] R. Sengodan, B. Chandar Shekar, R. Balamurugan, R. Kannan, R. Ranjith Kumar, J. Optoelectron. Adv. M. **19**(9-10), 595 (2017).

*Corresponding author: sengodan.r.sci@kct.ac.in